(14) C. K. Poon, *Coord. Chem. Rev.*, **16**, 1 (1973).
(15) National Academy of Science, "Critical Tables", McGraw-Hill, New York, N.Y., 1933.
(16) T. Beugelsdijk and R. Drago, *J. Am. Chem. Soc.*, **97**, 6466 (1975).
(17) The solubility of O_2 in DMF at 25.0 °C $p(O_2)$ = 760 mm, was taken to be 7.1×10^{-3} *m*: G. McLendon, unpublished determination.
(18) G. McLendon, S. Pickens, and A. Martell, *Inorg. Chem.*, **16**, 1551 (1977).
(19) While solvent is important in determining stoichiometry, the Co–cyclam system forms a binuclear complex in DMF as well as in H_2O. Thus solvation in this case only modifies an underlying electronic difference.
(20) It should be noted that the position and intensity ($\epsilon \sim 750$ at 80 K) are not inconsistent with an MCCT assignment.
(21) The $[CoMe_6(14)diene]^{2+}$ complex is a yellow low-spin species before oxygenation.

Contribution from the Department of Chemistry, University of Hawaii, Honolulu, Hawaii 96822

Crystal and Molecular Structure of Tris(ethylenediamine)nickel(II) Tetraphenylborate–Tris(dimethyl sulfoxide), $[Ni(NH_2CH_2CH_2NH_2)_3][B(C_6H_5)_4]_2 \cdot 3(CH_3)_2SO$. Factors Influencing the Ring Conformations in Tris(ethylenediamine) Metal Complexes

ROGER E. CRAMER* and JAMES T. HUNEKE[1]

Received March 2, 1977

The crystal structure of tris(ethylenediamine)nickel(II) tetraphenylborate–tris(dimethyl sulfoxide), $[Ni(en)_3][B(C_6H_5)_4]_2 \cdot 3(CH_3)_2SO$, has been determined by single-crystal x-ray diffraction techniques. Data complete to $2\theta = 45°$ (Mo Kα radiation) were collected with a Syntex $P\bar{1}$ automated diffractometer. After least-squares refinement using anisotropic thermal parameters only for the cation and solvates, the conventional R index converged at 0.092. The purple crystals form in the monoclinic space group $P2_1/a$ with $a = 23.51$ (4) Å, $b = 30.14$ (7) Å, $c = 9.910$ (8) Å, $\beta = 120.2$ (1)°, and $Z = 4$. The divalent nickel ion is hexacoordinated and exhibits the usual distortion from octahedral symmetry found in tris(ethylenediamine) complexes with an average twist angle of 50.7 ± 1.5° between the trigonal planes formed by the coordinated nitrogen atoms. The centric cell contains complex cations in both the $\Delta\lambda\lambda\delta$ and $\Lambda\delta\delta\lambda$ configurations. The tetraphenylborate anions are distorted in that the boron centers are found to deviate as much as 0.24 Å from atomic planes defined by the phenyl rings. A limited network of hydrogen bonding exists between the cation and the dimethyl sulfoxide solvate molecules. Inversion disorder at one of the sulfur atoms is observed. The $\Lambda\delta\delta\lambda$ mixed ring conformation found for the tris(ethylenediamine)nickel(II) complex in this structure confirms a previous spectroscopic characterization of the compound. An extensive analysis of other crystal structures of $[M(en)_3]^{m+}$ complexes is presented. The ring geometry observed in each compound is correlated with such parameters as intermolecular hydrogen bonding and anion size. It is suggested that the $\Lambda\delta\delta\lambda$ configuration is the lowest energy isomer for these complex cations.

Introduction

Five-membered ethylenediamine chelate rings have two possible conformations known as δ and λ. When three such chelates form a tris complex, the metal center is chiral and will have two possible enantiomeric configurations known as Δ and Λ. Combining all the structural possibilities there results, even for the simple, symmetrical chelate ethylenediamine (en), a total of eight isomers:[2] $\Lambda\delta\delta\delta$, $\Lambda\delta\delta\lambda$, $\Lambda\delta\lambda\lambda$, $\Lambda\lambda\lambda\lambda$, $\Delta\delta\delta\delta$, $\Delta\delta\delta\lambda$, $\Delta\delta\lambda\lambda$, $\Delta\lambda\lambda\lambda$. In a nonchiral medium the discussion can be limited to the first four of these isomers with the realization that all arguments apply equally well to their appropriate mirror images.

Examples of each isomer have been reported as a result of x-ray crystallographic investigations. In agreement with theoretical energy calculations,[3] the $\Lambda\delta\delta\delta$ isomer has been found to be the most abundant. More recently, however, it has been argued that hydrogen bonding[4] or crystal packing forces[5] may cause any of the four isomers to be the most stable. It has also been argued that entropy effects would cause the $\Lambda\delta\delta\lambda$ isomer to have the lowest free energy.[6] In order to test this latter contention it would be necessary to determine the structure of a $[M(en)_3]^{m+}$ complex ion in the presence of a large, nonhydrogen bonding counterion. The tetraphenylborate anion fulfills these criteria, and infrared spectroscopy had indicated that the ring conformations in $[Ni(en)_3][B(C_6H_5)_4]_2$ were mixed.[7] We have therefore determined the structure of this compound by x-ray methods and in this paper we report the results of that investigation.

Experimental Section

Preparation of $[Ni(en)_3][B(C_6H_5)_4]_2$. Tris(ethylenediamine)-nickel(II) chloride, $[Ni(en)_3]Cl_2$, was prepared by adding excess ethylenediamine to an aqueous solution of nickel chloride. When the product precipitated from solution upon addition of acetone, it was immediately filtered and dried. The $B(C_6H_5)_4^-$ salt was prepared by dissolving $[Ni(en)_3]Cl_2$ in H_2O and adding a $NaB(C_6H_5)_4$ solution. The product precipitated as a light purple powder which was filtered, washed, and dried. Chemical analyses were in close agreement with the expected values and the vibrational spectrum of $[Ni(en)_3][B(C_6H_5)_4]_2$ has been well characterized.[7] Electronic spectra obtained on Cary Model 14 showed absorption maxima for $[Ni(en)_3][B(C_6H_5)_4]_2$ in Me_2SO at 1.87, 1.27, and 1.14 μm^{-1}. $[Ni(en)_3]Cl_2$ in water gave bands at 1.85, 1.28, and 1.13 μm^{-1}. The literature values for solid $[Ni(en)_3](ClO_4)$ are 1.83, 1.27, and 1.12 μm^{-1}.[8]

Collection and Reduction of X-Ray Intensity Data Long, dark purple crystals of $[Ni(en)_3][B(C_6H_5)_4]_2 \cdot 3(CH_3)_2SO$ were obtained after a second slow recrystallization from a dimethyl sulfoxide solution at 23 °C. A well-formed crystal of original dimensions 0.06 × 0.21 × 3.25 mm was selected under a microscope and cleaved at both ends with a blade to give final dimensions of 0.06 × 0.21 × 0.33 mm. The six-sided, rectangular crystal was cemented using epoxy resin to the end of glass filament in such a way that the long edges of the crystal were nearly parallel to the filament.

A Syntex four-circle computer-controlled diffractometer with graphite monochromatized Mo Kα radiation (Kα_1, λ 0.709 26 Å; Kα_2, λ 0.71354 Å) and with a pulse height analyzer was used for preliminary experiments and for the measurement of diffraction intensities. The cell constants and their standard deviations were determined by a least-squares treatment of the angular coordinates of 15 independent reflections with 2θ values up to 21°. The cell constants at 20 °C for $[Ni(en)_3][B(C_6H_5)_4]_2 \cdot 3(CH_3)_2SO$ are $a = 23.51$ (4) Å, $b = 30.14$ (7) Å, $c = 9.910$ (8) Å, $\beta = 120.2$ (1)°, and $V = 6070$ (20) Å^3. The compound crystallizes in a monoclinic lattice with $P2_1/a$ symmetry and four molecules per unit cell. The calculated density $\rho_c = 1.216$ (7) g cm^{-3} is in good agreement with the density measured by flotation in a carbon tetrachloride–hexane solution of $\rho_m = 1.215$ (2) g cm^{-3}.

Diffraction intensities were collected by the θ–2θ scan technique at a scan rate varying from 2°/min in 2θ to 24°/min. A time equal to half the scan time for each reflection was spent counting the

0020-1669/78/1317-0365$01.00/0 © 1978 American Chemical Society

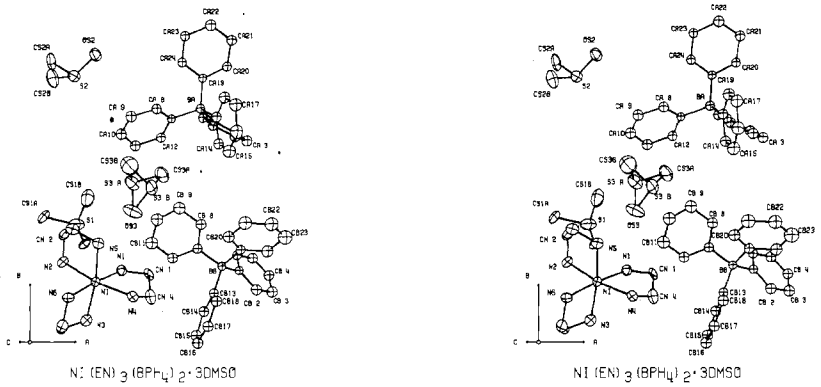

Figure 1. A stereoview of the asymmetric unit of $[Ni(en)_3][B(C_6H_5)_4]_2 \cdot 3Me_2SO$; the atom labeling is consistent with that in the tables. Ellipsoids of 20% probability are used. Both disordered positions of S3 are shown. (C. K. Johnson, ORTEP, Report ORNL-3794, Oak Ridge National Laboratory, Oak Ridge, Tenn., 1965.)

background at each end of the scan range, and standard deviations were assigned as previously described.[5] Fluctuations in the coolant water pressure automatically caused termination of the x-ray source three different times during data collection. As a result, the data were retrieved in four segments and the net counts of each individual set were corrected for Lorentz and polarization effects.

A set of three check reflections (200, $\bar{4}03$, and $4\bar{3}0$) was measured after each 100 reflections during data collection and the average total change in intensity was less than 4%. Therefore no decay correction was performed.

All 8330 unique reciprocal lattice points for which $2\theta \leq 45°$ were examined and only the 2253 showing intensities greater than three times their standard deviations (σ) were used in the structure refinement. At a lower limit of 2.5σ some 2539 reflections were "observable" but the more conservative 3σ criterion was retained.

All of the data meeting the $3\sigma(I)$ requirement were corrected for absorption ($\mu = 4.69$ cm^{-1}) using the Cartesian coordinates of three points on each of the six crystal faces in order to approximate the crystal shape in a $6 \times 4 \times 6$ grid.[9] Transmission coefficients ranged from 0.9049 to 0.9679.

The principal computer programs used in this study were described previously.[10] Atomic scattering factors[11] for Ni^+, S^0, O^0, N^0, C^0, B^0, and H (bonded)[12] were used. The first two were corrected to account for the real part of the anomalous dispersion.[13]

Solution and Refinement. Data systematically absent met the conditions $0k0$ ($k = 2n + 1$) and $h0l$ ($h = 2n + 1$) which uniquely define $P2_1/a$ (C_{2h}^5) as the space group. The positions of the nickel ion and two sulfur atoms were easily resolved using a sharpened three-dimensional[14,15] Patterson function. Successive cycles of Fourier refinement using electron difference density maps with phases based initially on these three atoms revealed the location of the 72 other nonhydrogen atoms in the structure. Full-matrix least-squares refinement with isotropic thermal parameters for all 75 positions converged at $R_1 = 0.142$ and $R_2 = 0.154$ where R_1 and R_2 are defined as before.

A difference Fourier synthesis at this point revealed substantial electron density around one sulfur atom which was attributed to disorder. Two positions were assigned to this sulfur atom and were refined with their isotropic thermal parameters fixed at 11.0 Å^2 but with variable occupancy values. Convergence was reached at $R_1 = 0.117$ and $R_2 = 0.124$ with occupancy values of 63 and 37%, respectively, for the sulfur atoms labeled as S3A and S3B.

Three successive cycles of least-squares refinement using anisotropic thermal parameters for the 26 atomic positions of the cation and the Me_2SO molecules and isotropic thermal parameters for the 50 atoms of two tetraphenylborate anions resulted in parameter shifts which were less than one-fourth of their standard deviations. Finally, the 24 hydrogen positions of the chelates were calculated[16] using a bond distance[17] of 0.95 Å and included in the structure factor calculation. Since the decrease in R_2 was found to be insignificant,[18] the hydrogen atom positions were not used in the final structure factor calculation.

A final difference Fourier synthesis had an estimated standard deviation in electron density of 0.10 e/Å^3 and revealed one area of residual electron density equal to 0.75 e/Å^3 near the sulfur atom S2. Occupancy refinement of the S2 position when $\beta = 8.25$ Å^2 gave a final value of 96% which may indicate a slight tendency for S2 to be disordered similar to S3. In the final structure factor calculation the occupancy of S2 was set equal to 1. All other peaks in this difference map were less than 0.50 e/Å^3.

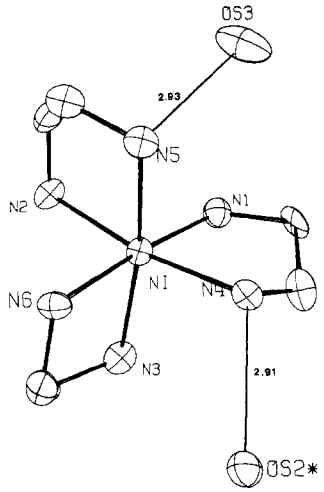

Figure 2. A view (ORTEP) of the $[Ni(en)_3]^{2+}$ coordination sphere showing the $\Lambda\delta\delta\lambda$ configuration and the two strong hydrogen bonds to dimethyl sulfoxide oxygens. Ellipsoids of 20% probability are used.

The final calculation of the structure factors and error functions yielded $R_1 = 0.092$ and $R_2 = 0.096$. The goodness of fit, $\{[\sum w(F_o - |F_c|)^2]/(m - s)\}^{1/2}$, is 1.07. The number of reflections $m = 2253$ and the total parameter number $s = 437$ give an overdetermination ratio of 5.16. The weighting factor, w, is given by $4F_o^2/\sigma^2(F_o^2)^2$ where σ represents the standard deviation.

The final positional and thermal parameters for the atoms refined anisotropically are given in Table I. Table II lists the positional and thermal parameters for the isotropically refined atoms. Bond lengths are given in Table III while Table IV contains bond angles. A listing of observed and calculated structure factors is also available.[19] A stereoview of the asymmetric unit is shown in Figure 1. Figure 2 illustrates a metal ion with the $\Lambda\delta\delta\lambda$ configuration. Figure 3 gives a stereoview of the contents of one unit cell. The numbering scheme for the atoms in the tables is consistent with that used in the figures.

Description of the Structure

All of the refined atoms of asymmetric unit are shown in Figure 1. Each of the three ethylenediamine ligands acts as a bidentate chelate and the six coordinating nitrogens form a distorted octahedron centered around the divalent nickel ion. The average chelate bite distance of 2.78 ± 0.02 Å (the uncertainties in averaged values are shown with ± and represent the root-mean-square average of the σ's for each separate value as computed from FMLS data) effects a distortion by compressing to 80.8 ± 0.6° the average N–Ni–N angle within each ligand from the 90° value expected for pure

Table I. Positional and Anisotropic Thermal Parameters[a]

Atom	x	y	z	U_{11}	U_{22}	U_{33}	U_{12}	U_{13}	U_{23}
Ni	0.1993 (1)	0.1048 (1)	0.9204 (3)	0.048 (2)	0.060 (1)	0.035 (1)	0.002 (2)	0.0185 (9)	−0.001 (2)
N1	0.2235 (8)	0.1272 (5)	0.751 (2)	0.06 (1)	0.074 (9)	0.06 (1)	−0.003 (9)	0.03 (1)	−0.005 (9)
N2	0.1064 (7)	0.1407 (6)	0.798 (2)	0.06 (1)	0.07 (1)	0.04 (1)	0.019 (9)	0.019 (9)	−0.001 (9)
N3	0.1594 (8)	0.0418 (6)	0.811 (2)	0.06 (1)	0.09 (1)	0.04 (1)	0.008 (9)	0.007 (9)	−0.003 (9)
N4	0.2966 (7)	0.0794 (5)	1.026 (2)	0.06 (1)	0.064 (9)	0.02 (1)	0.000 (8)	0.017 (9)	0.015 (7)
N5	0.2287 (8)	0.1653 (5)	1.045 (2)	0.07 (1)	0.074 (9)	0.04 (1)	−0.006 (9)	0.016 (9)	−0.009 (9)
N6	0.1755 (8)	0.0765 (6)	1.087 (2)	0.09 (1)	0.051 (9)	0.05 (1)	0.000 (9)	0.04 (1)	0.005 (9)
CN1	0.293 (1)	0.1200 (8)	0.808 (3)	0.10 (2)	0.08 (2)	0.09 (2)	−0.03 (1)	0.08 (2)	0.00 (2)
CN2	0.119 (1)	0.1859 (9)	0.846 (4)	0.07 (2)	0.08 (2)	0.11 (3)	0.02 (1)	0.04 (2)	−0.01 (2)
CN3	0.118 (1)	0.0260 (7)	0.874 (4)	0.08 (2)	0.05 (1)	0.12 (3)	−0.01 (1)	0.06 (2)	0.00 (1)
CN4	0.313 (1)	0.080 (1)	0.902 (3)	0.07 (2)	0.14 (3)	0.08 (2)	−0.01 (2)	0.04 (2)	0.00 (2)
CN5	0.168 (2)	0.1898 (8)	1.010 (4)	0.10 (2)	0.08 (2)	0.08 (2)	−0.01 (2)	0.04 (2)	0.00 (2)
CN6	0.155 (1)	0.0305 (8)	1.045 (3)	0.09 (2)	0.10 (2)	0.08 (2)	0.03 (1)	0.06 (2)	0.05 (2)
S1	0.0548 (5)	0.2182 (3)	0.389 (1)	0.17 (1)	0.087 (5)	0.169 (9)	0.006 (6)	0.071 (7)	0.002 (6)
OS1	0.0913 (7)	0.1803 (5)	0.481 (2)	0.09 (1)	0.064 (9)	0.15 (2)	0.039 (9)	0.06 (1)	0.02 (1)
CS1A	−0.006 (2)	0.230 (1)	0.457 (5)	0.16 (3)	0.10 (2)	0.32 (5)	0.05 (2)	0.17 (3)	0.02 (3)
CS1B	0.098 (2)	0.262 (2)	0.482 (4)	0.11 (3)	0.25 (5)	0.17 (3)	−0.02 (3)	0.07 (2)	−0.08 (3)
S2	0.1392 (4)	0.4529 (2)	0.851 (1)	0.128 (6)	0.087 (5)	0.159 (8)	−0.026 (5)	0.097 (6)	−0.027 (5)
OS2	0.1970 (8)	0.4843 (5)	0.917 (2)	0.069 (8)	0.092 (9)	0.11 (1)	0.00 (1)	0.035 (8)	0.01 (1)
CS2A	0.067 (1)	0.486 (1)	0.736 (3)	0.05 (1)	0.16 (2)	0.14 (2)	0.01 (2)	0.05 (2)	0.05 (2)
CS2B	0.125 (1)	0.438 (1)	1.001 (3)	0.09 (2)	0.19 (3)	0.09 (2)	−0.02 (2)	0.04 (2)	0.02 (2)
S3A	0.2660 (8)	0.2731 (5)	0.859 (2)	0.11 (1)	0.120 (9)	0.13 (1)	−0.017 (9)	0.04 (1)	0.025 (9)
S3B	0.323 (1)	0.2613 (8)	0.953 (3)	0.06 (1)	0.12 (2)	0.15 (2)	0.03 (1)	0.03 (2)	0.07 (2)
OS3	0.270 (1)	0.2244 (7)	0.875 (3)	0.24 (3)	0.11 (2)	0.15 (2)	−0.07 (2)	0.11 (2)	−0.02 (1)
CS3A	0.321 (2)	0.290 (1)	0.810 (5)	0.20 (3)	0.15 (3)	0.24 (4)	−0.05 (3)	0.17 (3)	−0.01 (3)
CS3B	0.294 (2)	0.293 (2)	1.051 (5)	0.22 (4)	0.21 (4)	0.19 (4)	−0.05 (3)	0.14 (4)	−0.06 (4)

[a] The form of the anisotropic thermal ellipsoid is $\exp[-2\pi^2(U_{11}h^2a^{*2} + U_{22}k^2b^{*2} + U_{33}l^2c^{*2} + 2U_{12}hka^*b^* + 2U_{13}hla^*c^* + 2U_{23}klb^*c^*)]$.

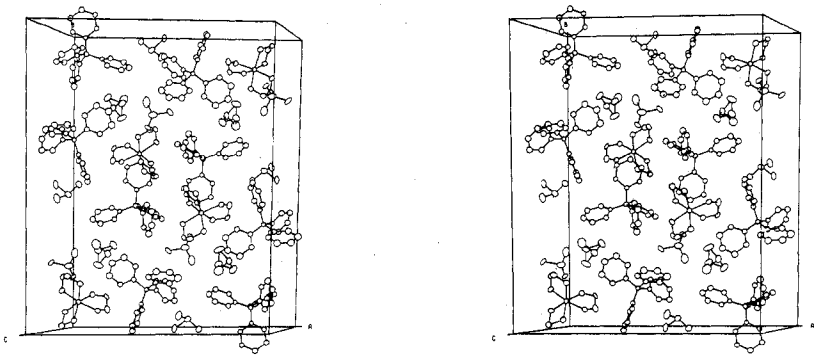

Figure 3. A stereoview (ORTEP) of the contents of a unit cell of $[Ni(en)_3][B(C_6H_5)_4]_2 \cdot 3Me_2SO$. Ellipsoids of 20% probability are used.

octahedral symmetry. The distorted octahedron of coordinating nitrogens is actually a trigonal antiprism[20] in which the average twist angle between the trigonal planes defined by N1–N2–N3 and N4–N5–N6 is 50.7 ± 1.5°.

The five-membered rings formed by each chelate are not flat. The parameter ω, the dihedral angle between the planes defined, for example, by N1–CN1–CN4 and CN1–CN4–N4, has been suggested[21] as a measure of ring pucker. The ω value for both the N1–N4 and N2–N5 rings is 52.6 ± 2.0°, while the chelate ring N3–N6 has ω = 57 (2)°. These values compare with ω = 56° calculated for $[Ni(en)_3]SO_4$[21] and ω = 50.4 ± 1.0° found in $[Ni(en)_3](O_2C_2H_3)_2 \cdot 2H_2O$.[5]

The chelate ring conformations found in this complex are illustrated in Figure 2. The configuration about the metal center presented there is Λ with both the N2–N5 and N3–N6 chelates present in the δ conformation so that the C2–C5 and C3–C6 bond vectors are parallel to the pseudo-C_3 axis of the complex ion. The N1–N4 ring, however, is present as the λ conformer with the C1–C4 bond vector forming an oblique angle with the pseudo-C_3 axis of the complex ion. The complete configuration of the cation illustrated in Figure 2 is Λδδλ. Because of the symmetry of the crystal there are an equal number of Λδδλ and Δλλδ configurations positioned in pairs across inversion centers in the unit cell. The Λδδλ configuration found with the tetraphenylborate ion in this structure confirms the ability of the technique we have described previously[7] to detect mixed ring configurations using vibrational spectroscopy.

The tetraphenylborate anions occur in this structure with certain distortions that are analogous to those found in other reported structures.[22,23] For example, the bond lengths in Table III are not significantly different from reported values and, in like manner, some of the carbon–boron–carbon angles in Table IV deviate slightly from true tetrahedral geometry. Furthermore, as the data in Table V point out, in most cases the boron atom does not lie in the least-squares planes of the phenyl rings. The boron atoms, BA and BB, deviate on the average 0.118 ± 0.017 and 0.105 ± 0.017 Å, respectively, from the planes of the phenyl rings of anions A and B. This can be compared to an average value of 0.12 Å found for the tetraphenylborate anion in the structure[22] of $[Ni_2(tren)_2(OCN)_2][B(C_6H_5)_4]_2$.

The positions of the dimethyl sulfoxide solvates are illustrated in Figures 1 and 3. Each of these molecules has a trigonal-pyramidal geometry with intraatomic angles roughly approximating tetrahedral values. The data given in Tables III and IV for these molecules do not differ significantly from the values found for other crystal structures involving dimethyl sulfoxide as a solvate[24,25] or from the structure of crystalline Me_2SO.[26,27]

The disorder at sulfur atom S3 can be best described as a pyramidal inversion[28] in which the basal plane formed by

Table II. Isotropic Atom Positions and Thermal Parameters[a]

Atom	x	y	z	U_{iso}, Å²
BA	3635 (11)	4207 (7)	5408 (27)	5.7 (6)
CA1	3721 (8)	4078 (6)	3868 (21)	5.4 (5)
CA2	4263 (9)	3849 (6)	3950 (23)	6.7 (6)
CA3	4307 (10)	3800 (7)	2559 (27)	8.0 (6)
CA4	3824 (10)	3961 (8)	1146 (25)	8.5 (6)
CA5	3270 (9)	4176 (6)	1026 (25)	7.0 (6)
CA6	3222 (9)	4233 (6)	2367 (24)	6.0 (5)
CA7	2940 (8)	4032 (6)	5218 (19)	4.6 (5)
CA8	2811 (9)	4127 (6)	6416 (23)	6.5 (6)
CA9	2229 (10)	3997 (7)	6344 (24)	7.6 (6)
CA10	1784 (11)	3758 (7)	5079 (29)	8.2 (8)
CA11	1885 (10)	3621 (7)	3846 (26)	7.9 (6)
CA12	2503 (10)	3767 (6)	4001 (24)	6.6 (6)
CA13	4232 (8)	3958 (7)	7057 (22)	6.3 (5)
CA14	4284 (9)	3487 (7)	7048 (25)	6.8 (6)
CA15	4736 (12)	3280 (8)	8555 (32)	10.0 (8)
CA16	5074 (12)	3542 (8)	9847 (31)	9.6 (8)
CA17	5059 (11)	3984 (9)	9882 (27)	9.2 (6)
CA18	4616 (11)	4200 (7)	8428 (28)	8.0 (6)
CA19	3699 (8)	4741 (5)	5540 (21)	4.8 (5)
CA20	4288 (9)	4936 (6)	5806 (21)	5.7 (5)
CA21	4412 (9)	5390 (7)	5965 (23)	6.8 (6)
CA22	3930 (10)	5661 (7)	5881 (25)	8.0 (6)
CA23	3299 (9)	5488 (6)	5560 (22)	5.8 (5)
CA24	3201 (8)	5033 (6)	5346 (21)	5.6 (5)
BB	4118 (10)	1396 (7)	5341 (26)	4.8 (6)
CB1	4312 (8)	1354 (6)	3886 (22)	5.2 (5)
CB2	4726 (10)	1005 (8)	3967 (24)	8.0 (6)
CB3	4952 (10)	980 (8)	2838 (27)	8.5 (6)
CB4	4738 (10)	1309 (7)	1755 (27)	7.7 (6)
CB5	4326 (10)	1632 (7)	1633 (26)	7.7 (6)
CB6	4097 (9)	1663 (6)	2703 (23)	6.0 (5)
CB7	3474 (9)	1724 (6)	4767 (24)	6.5 (6)
CB8	3526 (10)	2167 (7)	4615 (26)	7.9 (6)
CB9	2977 (13)	2478 (9)	4264 (30)	10.4 (8)
CB10	2406 (13)	2279 (9)	3920 (31)	10.9 (9)
CB11	2313 (13)	1845 (9)	4097 (31)	10.8 (9)
CB12	2858 (10)	1561 (7)	4464 (24)	7.2 (6)
CB13	4006 (8)	912 (6)	5826 (21)	5.6 (5)
CB14	3603 (10)	602 (7)	4616 (25)	7.3 (6)
CB15	3484 (10)	167 (7)	4964 (27)	7.6 (6)
CB16	3756 (10)	32 (7)	6512 (27)	8.0 (6)
CB17	4156 (10)	317 (7)	7681 (25)	7.1 (6)
CB18	4291 (10)	753 (7)	7374 (25)	7.2 (6)
CB19	4757 (9)	1650 (6)	6899 (23)	6.2 (5)
CB20	4648 (11)	1844 (7)	7993 (27)	8.1 (6)
CB21	5199 (13)	2033 (9)	9442 (31)	10.9 (8)
CB22	5791 (13)	2010 (9)	9616 (32)	10.8 (8)
CB23	5961 (14)	1821 (10)	8609 (38)	13 (1)
CB24	5381 (12)	1623 (8)	7094 (28)	9.0 (8)

[a] Fractional coordinates × 10^4 and U_{iso} × 10^2 are given. The esd is in the units of the least significant digit given for the corresponding parameter.

atoms OS3, CS3A, and CS3B finds its pyramidal apex at position S3A in 63% of the unit cells and at position S3B in 37% of the unit cells. The calculated data listed for plane 9 in Table V clearly show that the two sulfur positions are equidistant from this basal plane. Also, the S3A–S3B distance of 1.23 (3) Å given in Table III agrees quite well with the value 1.24 Å calculated by inverting a geometric model using angles and distances of the S3A dimethyl sulfoxide molecule.

Intermolecular Interactions

Listed in Table VI are all possible interactions between Lewis base sites and the amine nitrogens of the chelates for which the distance is less than 3.50 Å. Among these are two which can be considered as strong hydrogen bonds because of their short distances plus a directed angle near 180°. In all cases it is the oxygen atoms of Me_2SO molecules, particularly OS2 and OS3, which form hydrogen bonds with amine protons. The two strong interactions at distances less than 3.0 Å have been included in Figure 2 where only the oxygen atoms of the respective Me_2SO molecules have been depicted.

Table III. Bond Distances (A) and Standard Deviations

Coordination Sphere		Solvates	
Ni-N1	2.14 (2)	S1-OS1	1.45 (2)
Ni-N2	2.18 (1)	S1-CS1A	1.90 (4)
Ni-N3	2.16 (2)	S1-CS1B	1.64 (4)
Ni-N4	2.12 (1)	S2-OS2	1.51 (2)
Ni-N5	2.11 (2)	S2-CS2A	1.80 (3)
Ni-N6	2.17 (1)	S2-CS2B	1.75 (3)
Chelate Rings		S3A-OS3	1.48 (3)
N1-CN1	1.45 (3)	S3A-CS3A	1.67 (4)
N2-CN2	1.42 (3)	S3A-CS3B	1.77 (5)
N3-CN3	1.47 (3)	S3B-OS3	1.55 (3)
N4-CN4	1.46 (3)	S3B-CS3A	1.64 (5)
N5-CN5	1.48 (3)	S3B-CS3B	1.72 (5)
N6-CN6	1.46 (3)	S3A-S3B	1.23 (3)
CN1-CN4	1.44 (4)		
CN2-CN5	1.45 (4)		
CN3-CN6	1.47 (4)		
Tetraphenylborate Anions			
BA-CA1	1.68 (3)	BB-CB1	1.72 (3)
BA-CA7	1.63 (3)	BB-CB7	1.65 (3)
BA-CA13	1.70 (3)	BB-CB13	1.60 (3)
BA-CA19	1.61 (3)	BB-CB19	1.70 (3)
CA1-CA2	1.41 (2)	CB1-CB2	1.41 (3)
CA2-CA3	1.44 (3)	CB2-CB3	1.46 (3)
CA3-CA4	1.37 (3)	CB3-CB4	1.36 (3)
CA4-CA5	1.41 (3)	CB4-CB5	1.34 (3)
CA5-CA6	1.40 (3)	CB5-CB6	1.41 (3)
CA6-CA1	1.43 (3)	CB6-CB1	1.38 (3)
CA7-CA8	1.40 (2)	CB7-CB8	1.35 (3)
CA8-CA9	1.39 (3)	CB8-CB9	1.49 (3)
CA9-CA10	1.37 (3)	CB9-CB10	1.35 (4)
CA10-CA11	1.42 (3)	CB10-CB11	1.35 (4)
CA11-CA12	1.45 (3)	CB11-CB12	1.43 (3)
CA12-CA7	1.38 (2)	CB12-CB7	1.41 (3)
CA13-CA14	1.43 (3)	CB13-CB14	1.44 (3)
CA14-CA15	1.47 (3)	CB14-CB15	1.42 (3)
CA15-CA16	1.37 (4)	CB15-CB16	1.39 (3)
CA16-CA17	1.33 (4)	CB16-CB17	1.37 (3)
CA17-CA18	1.44 (3)	CB17-CB18	1.42 (3)
CA18-CA13	1.40 (3)	CB18-CB13	1.41 (3)
CA19-CA20	1.40 (2)	CB19-CB20	1.36 (3)
CA20-CA21	1.39 (3)	CB20-CB21	1.48 (3)
CA21-CA22	1.37 (3)	CB21-CB22	1.31 (4)
CA22-CA23	1.45 (3)	CB22-CB23	1.37 (4)
CA23-CA24	1.39 (3)	CB23-CB24	1.55 (4)
CA24-CA19	1.40 (2)	CB24-CB19	1.38 (3)

Several van der Waals contacts exist between methylene and phenyl carbon centers. Pauling[29] sets the limit of this type of interaction at 2.0 ± 1.7 = 3.7 Å and most of the distances we have found are approximately 3.6 Å. For example, in Figure 1 the distance from CN4 to CB17 is 3.60 Å. However, a short contact, 3.48 Å, occurs between CB15 in Figure 1 and a CN2 position at $^1/_2 + x$, $^1/_2 - y$, z. Also, methyl carbon CS3A approaches to within 3.6 Å of phenyl carbons CA14 and CA15.

Discussion of the Results

This is the first example of the Λδδλ isomer in a Ni(II) complex. The large, nonhydrogen bonding $[B(C_5H_6)_4]^-$ counterions minimize the possible Lewis acid type interactions of the amine groups on the cation. As a result there are only two strong hydrogen bonds, both to Me_2SO solvates, in this structure. These are the fewest hydrogen bonds ever reported for a $[M(en)_3]^{m+}$ complex. The only other report of the Λδδλ isomer is the structure of $[Cr(en)_3][Ni(CN)_5]\cdot 1.5H_2O$[30] in which only three strong hydrogen bonds exist. The similarity of the hydrogen bonding in these two structures can be seen by examining Figures 2 and 4.

A survey (Table VII) of the hydrogen bonding in other crystal structures involving the $[M(en)_3]^{m+}$ cation shows that

Table IV. Bond Angles (deg) and Standard Deviations

	Coordination Sphere		
N1-Ni-N2	89.7 (0.6)	N2-Ni-N6	92.8 (0.6)
N1-Ni-N3	95.9 (0.6)	N3-Ni-N4	91.0 (0.6)
N1-Ni-N4	81.7 (0.6)	N3-Ni-N5	170.5 (0.6)
N1-Ni-N5	92.9 (0.6)	N3-Ni-N6	79.8 (0.6)
N1-Ni-N6	175.2 (0.6)	N4-Ni-N5	93.9 (0.6)
N2-Ni-N3	95.5 (0.6)	N4-Ni-N6	96.2 (0.6)
N2-Ni-N4	169.7 (0.6)	N5-Ni-N6	91.6 (0.6)
N2-Ni-N5	80.8 (0.6)		
	Chelate Rings		
Ni-N1-CN1	109.7 (1.3)	N1-CN1-CN4	108.4 (2.0)
Ni-N2-CN2	108.1 (1.5)	N2-CN2-CN5	111.6 (2.1)
Ni-N3-CN3	106.5 (1.3)	N3-CN3-CN6	108.9 (2.4)
Ni-N4-CN4	104.4 (1.5)	N4-CN4-CN1	115.1 (1.9)
Ni-N5-CN5	107.4 (1.3)	N5-CN5-CN2	111.5 (2.1)
Ni-N6-CN6	109.0 (1.4)	N6-CN6-CN3	109.9 (1.9)
	Solvates		
CS1A-S1-CS1B	91.2 (1.9)	CS3A-S3A-CS3B	107.0 (2.1)
OS1-S1-CS1A	103.6 (1.6)	OS3-S3A-CS3A	108.3 (1.9)
OS1-S1-CS1B	106.6 (1.5)	OS3-S3A-CS3B	104.2 (1.9)
CS2A-S2-CS2B	99.2 (1.5)	CS3A-S3B-CS3B	110.9 (2.4)
OS2-S2-CS2A	106.3 (1.1)	OS3-S3B-CS3A	106.1 (2.3)
OS2-S2-CS2B	108.4 (1.2)	OS3-S3B-CS3B	103.3 (2.1)
	Tetraphenylborate Anions		
CA1-BA-CA7	113.0 (1.5)	CB1-BB-CB7	109.8 (1.4)
CA1-BA-CA13	110.6 (1.5)	CB1-BB-CB13	109.7 (1.5)
CA1-BA-CA19	104.8 (1.5)	CB1-BB-CB19	108.1 (1.4)
CA7-BA-CA13	105.2 (1.5)	CB7-BB-CB13	112.8 (1.6)
CA7-BA-CA19	112.2 (1.6)	CB7-BB-CB19	106.4 (1.5)
CA13-BA-CA19	111.3 (1.6)	CB13-BB-CB19	109.9 (1.5)
CA1-CA2-CA3	119.4 (1.7)	CB1-CB2-CB3	120.2 (1.8)
CA2-CA3-CA4	121.3 (1.9)	CB2-CB3-CB4	115.7 (1.9)
CA3-CA4-CA5	120.3 (2.0)	CB3-CB4-CB5	124.6 (2.1)
CA4-CA5-CA6	119.4 (1.8)	CB4-CB5-CB6	120.8 (2.0)
CA5-CA6-CA1	122.0 (1.7)	CB5-CB6-CB1	118.6 (1.7)
CA6-CA1-CA2	117.5 (1.6)	CB6-CB1-CB2	120.0 (1.7)
CA7-CA8-CA9	121.9 (1.8)	CB7-CB8-CB9	122.0 (2.0)
CA8-CA9-CA10	118.4 (2.0)	CB8-CB9-CB10	114.5 (2.3)
CA9-CA10-CA11	124.1 (2.0)	CB9-CB10-CB11	127.1 (2.6)
CA10-CA11-CA12	114.5 (1.8)	CB10-CB11-CB12	115.5 (2.4)
CA11-CA12-CA7	122.3 (1.8)	CB11-CB12-CB7	122.6 (2.0)
CA12-CA7-CA8	118.5 (1.6)	CB12-CB7-CB8	117.4 (1.9)
CA13-CA14-CA15	116.0 (1.9)	CB13-CB14-CB15	121.7 (1.8)
CA14-CA15-CA16	119.3 (2.2)	CB14-CB15-CB16	120.0 (1.9)
CA15-CA16-CA17	126.2 (2.3)	CB15-CB16-CB17	119.2 (1.9)
CA16-CA17-CA18	116.2 (2.1)	CB16-CB17-CB18	122.2 (1.9)
CA17-CA18-CA13	121.6 (1.9)	CB17-CB18-CB13	120.8 (1.8)
CA18-CA13-CA14	120.7 (1.7)	CB18-CB13-CB14	116.0 (1.6)
CA19-CA20-CA21	124.4 (1.7)	CB19-CB20-CB21	120.9 (2.0)
CA20-CA21-CA22	117.5 (1.9)	CB20-CB21-CB22	117.3 (2.4)
CA21-CA22-CA23	121.6 (1.9)	CB21-CB22-CB23	127.1 (2.7)
CA22-CA23-CA24	117.5 (1.7)	CB22-CB23-CB24	115.3 (2.4)
CA23-CA24-CA19	122.5 (1.7)	CB23-CB24-CB19	117.8 (2.1)
CA24-CA19-CA20	116.1 (1.6)	CB24-CB19-CB20	121.6 (1.9)

these two examples of the $\Lambda\delta\delta\lambda$ isomer are found in the presence of the fewest strong hydrogen bonds. This observation implies that the $\Lambda\delta\delta\lambda$ configuration has the lowest free energy, in the absence of perturbations from the environment, in accord with the free energy calculations of Gollogly, Hawkins, and Beattie.[6]

If the $\Lambda\delta\delta\lambda$ isomer does have the lowest free energy, what are the factors which favor the stabilization of the higher energy $\Lambda\delta\delta\delta$, $\Lambda\delta\lambda\lambda$, and $\Lambda\lambda\lambda\lambda$ isomers? In an effort to discover these factors we have scrutinized the many other individual structural reports of $[M(en)_3]^{m+}$ cations which are available. The number and average distance of the various hydrogen bonds found in these structures are presented in Table VII. For the hydrogen bond acceptors involved we have used the limiting distances for strong hydrogen bonds established by Hamilton and Ibers.[31] In the case of $[Ni(en)_3](NO_3)_2$ where each proton forms a bifurcated hydrogen bond,[32] we have

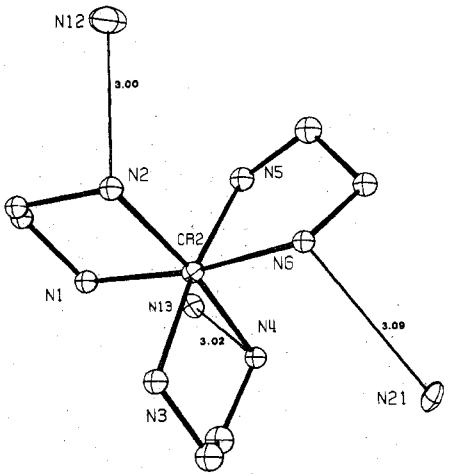

Figure 4. Hydrogen bonding to the $\Lambda\delta\delta\lambda$ configuration in $[Cr(en)_3][Ni(CN)_5] \cdot 1.5H_2O$.[30] Ellipsoids of 20% probability are used.

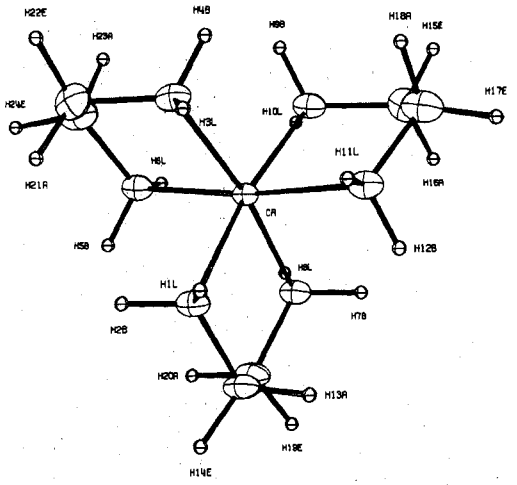

Figure 5. The coordination sphere including calculated hydrogen positions for the $\Lambda\delta\delta\delta$ cation in $[Cr(en)_3][MoO(OH)(CN)_4] \cdot H_2O$.[33] Bond lengths of 1.07 and 1.03 Å, respectively, for C–H and N–H were assumed. Amine hydrogens 1 through 12 are defined as lel or ob types and correspondingly labeled with L or B. Methylene hydrogens 13 through 24 are defined as equatorial or axial with E or A labels.

exceeded the maximum of 3.10 Å normally expected for a strong hydrogen bond.

The data in Table VII have been categorized first by the conformation of the ring δ or λ, to which the hydrogen bonding amine proton belongs, and second by the type of amine proton, lel or ob, which is involved in the hydrogen bond. We have distinguished these two types of amine protons (see Figure 5) by the orientation of the N–H bond vectors with respect to the pseudo-C_3 axis of the cation, which is normal to the plane of the page in Figures 1–5. An amine proton is called lel when its N–H bond vector is nearly parallel to the pseudo-C_3 axis while ob indicates one whose N–H vector forms an oblique angle with this axis. Previous workers[4] had referred to lel protons as "axial" and the ob protons as "equatorial". Their nomenclature, however, can be confused with the well-accepted designations axial and equatorial which are used to describe the inequivalent hydrogen positions in nonplanar ring systems. For example, proton H3L in Figure 5 is axial with respect to the C_3 axis of the complex, but it is equatorial with respect to the chelate ring. We therefore propose lel and ob as less confusing terminology.

A survey of Table VII reveals several correlations between the occurrence of particular ring conformations and the details

Table V. Deviations of Atoms from Least-Squares Planes (Å × 10^3)[a]

	Plane 1		Plane 2		Plane 3		Plane 4		Plane 5		Plane 6		Plane 7		Plane 8		Plane 9	
	CA1	*13*	CA7	*−27*	CA13	*14*	CA19	*27*	CB1	*17*	CB7	*7*	CB13	*13*	CB19	*0*	OS3	*0*
	CA2	*−13*	CA8	*23*	CA14	*−10*	CA20	*−4*	CB2	*−9*	CB8	*−18*	CB14	*−6*	CB20	*0*	CS3A	*0*
	CA3	*2*	CA9	*3*	CA15	*−5*	CA21	*−20*	CB3	*−10*	CB9	*41*	CB15	*−8*	CB21	*3*	CS3B	*0*
	CA4	*12*	CA10	*−25*	CA16	*23*	CA22	*20*	CB4	*20*	CB10	*−47*	CB16	*17*	CB22	*−5*		
	CA5	*−7*	CA11	*0*	CA17	*−12*	CA23	*12*	CB5	*−3*	CB11	*26*	CB17	*−1*	CB23	*4*		
	CA6	*−4*	CA12	*27*	CA18	*−6*	CA24	*−32*	CB6	*−11*	CB12	*−6*	CB18	*−12*	CB24	*0*		
	BA	150	BA	−22	BA	237	BA	64	BB	166	BB	102	BB	14	BB	138	S3A	−617
																	S3B	613
$q_b \times c$	4549		2383		−9757		−1646		5664		−2235		−9416		−1073		6908	
q_b	8719		−8367		−695		−838		5677		1080		3351		−8820		−3551	
q_c	1813		4930		2072		9828		5974		9687		293		4587		6298	
D	14.41		−6.91		−5.87		2.46		8.94		3.22		−5.08		−2.50		3.69	
δ	10		21		13		22		13		29		11		3		0	

[a] Italic deviations indicate the atoms used to define the least-squares plane. A negative deviation from a plane indicates that the atom position lies between that plane and the origin. The direction cosines (×10^4), q, are with respect to orthogonal axes. D is the distance (in Å) from the plane to the origin as calculated in MOLGE. The root mean square of the italic deviations (Å × 10^3) from the plane is δ.

Table VI. Possible A–H···B Bonds with A···B Distances Less Than 3.50 Å

A	B[a]	A–B, Å	AHB,[b] deg
N1	OS1	3.32 (2)	119.3 (1.5)
N1	OS3	3.15 (3)	129.7 (1.6)
N2	OS1	3.21 (2)	131.3 (1.5)
N4	OS2*	2.91 (2)	155.7 (1.6)
N5	OS3	2.93 (3)	155.2 (1.7)

[a] OS2* is the coordinates of OS2 in Table I transformed to $^1/_2 - x, y - ^1/_2, 2 - z$. [b] Tetrahedral hydrogen positions were calculated using a N–H bond length of 0.95 Å.

of the hydrogen bonding schemes. The $\Lambda\delta\delta\delta$ configuration is the most plentiful. In addition, the hydrogen bonds to ob amine protons of the δ rings in these compounds, I through X, are greater in number or greater in strength than those to lel protons. In those compounds with λ rings, XI through XV, a similar comparison shows a reversal of this trend; i.e., in λ rings hydrogen bonds to lel protons tend to be either more abundant or stronger than those to ob protons. Also, in all those compounds having both δ and λ rings, the hydrogen bonds to the δ rings tend to be stronger. This conclusion is supported by previously reported Raman data,[7] where the shift from the ν(N–H) frequency of free ethylenediamine was nearly twice as large for the $\Lambda\delta\delta\delta$ isomers as for compounds containing some λ rings. While it seems possible that these subtle differences may cause preferential stabilization of a particular isomer, it does not appear likely that a direct correlation exists simply between the total number of hydrogen bonds and the occurrence of λ rings. However, it is clear from this survey that the weakest amount of hydrogen bonding occurs only in the two examples of the $\Lambda\delta\delta\lambda$ configuration.

Since the $[Cr(en)_3]^{3+}$ ion has been found now in all four isomeric forms (compounds X, XII, and XIV in Table VII) it is possible to accurately and systematically compare the structural differences between the isomers. The hydrogen positions for each of the cations in this series of Cr(III) complexes were calculated[16] using bond distances of 1.07 and 1.03 Å,[17] resepctively, for the methylene and amine protons. Using these data we have evaluated certain geometrical aspects which could affect the stability of each particular isomer.

Earlier workers had suggested[4] that the change from the $\Lambda\delta\delta\delta$ to the $\Lambda\lambda\lambda\lambda$ configuration involves a general broadening of the metal complex. If the volumes of the four cation isomers differ greatly, then we might expect anion size to be an important parameter affecting the occurrence of particular isomers in the solid state. For example, Table VII reveals that λ ring conformations have been found only in those $[M(en)_3]^{m+}$ structures which involve rather large anions.

We attempted to calculate the volume of each of the four isomers of the Λ configuration. Our method involves calculating the volume of a 44-sided, irregular polyhedron called a tetracontatetrahedron formed by connecting adjacent hydrogen positions into sets of three each, so that 44 nonoverlapping triangles are formed. The triangular faces of the polyhedron were selected to be nearly equilateral and so that the overall resultant surface of the polyhedron was convex. Output from the molecular geometry program, MOLGE,[35] was used to obtain the area of the triangle formed by each set of three hydrogens along with the perpendicular distance from

Table VII. Average Amine Hydrogen Bond Distances, Å

			δ ring		λ ring		
No.	Compd	Λ[a]	lel	ob	lel	ob	Ref
I	(+)-$[Co(en)_3]Cl_3 \cdot H_2O$	$\delta\delta\delta$	2 (3.25)	4 (3.04)			42
II	(+)-$[Co(en)_3](NO_3)_3$	$\delta\delta\delta$	6 (3.05)	5 (3.01)			40
III	$[Co(en)_3]Cl_3 \cdot 3H_2O$	$\delta\delta\delta$	6 (3.22)	3 (3.13)			43
IV	(+)-$[Co(en)_3]Br_3 \cdot H_2O$	$\delta\delta\delta$	2 (3.34)	6 (3.16)			41
V	$[Co(en)_3]_2(HPO_4)_3 \cdot 9H_2O$	$\delta\delta\delta$	4 (2.85)	5 (2.95)			38
VI	$[Cu(en)_3]SO_4$	$\delta\delta\delta$	5 (2.98)	3 (2.89)			39
VII	$[Ni(en)_3]SO_4$	$\delta\delta\delta$	5 (2.98)	3 (2.89)			37
VIII	$[Ni(en)_3](NO_3)_2$	$\delta\delta\delta$	6 (3.24)	6 (3.25)			32
IX	$[Ni(en)_3](C_2H_3O_2)_2 \cdot 2H_2O$	$\delta\delta\delta$	3 (2.98)	2 (2.98)			5
X	$[Cr(en)_3][MoO(OH)(CN)_4]H_2O$	$\delta\delta\delta$	4 (2.91)	6 (3.05)			33
XI	$[Ni(en)_3][B(C_6H_5)_4]_2 \cdot 3(CH_3)_2SO$	$\delta\delta\lambda$		1 (2.93)		1 (2.91)	This work
XIIa	$[Cr(en)_3][Ni(CN)_5] \cdot 1.5H_2O$	$\delta\delta\lambda$		1 (3.00)	1 (3.02)	1 (3.09)	30
XIIb		$\delta\lambda\lambda$	1 (2.99)	2 (2.96)	4 (3.04)	1 (3.02)	
XIII	$[Co(en)_3]_2[Cu_2Cl_8]Cl_2 \cdot 2H_2O$	$\delta\lambda\lambda$	2 (3.19)	1 (2.84)			45
XIV	$[Co(en)_3][Cr(CN)_5NO] \cdot 2H_2O$	$\delta\lambda\lambda$		2 (3.01)	2 (3.01)	3 (3.03)	44
XV	$[Cr(en)_3][Co(CN)_6] \cdot 6H_2O$	$\lambda\lambda\lambda$			6 (2.96)	4 (3.03)	34

[a] Discussion has been limited to only one enantiotopic metal configuration.

Table VIII. Geometrical Considerations in the Four Unique Isomers of $[Cr(en)_3]^{3+}$

	$\Lambda\delta\delta\delta$[a]	$\Lambda\delta\delta\lambda$[b]	$\Lambda\delta\lambda\lambda$[b]	$\Lambda\lambda\lambda\lambda$[c]
Av M-N dist, Å	2.073 (5)	2.073 (7)	2.076 (3)	2.081 (9)
Height along C_3 axis, Å	4.278	4.207 (3)	4.115 (1)	4.073 (2)
Av radius (from C_3 axis to 6 H_{eq}'s), Å	3.873 (3)	3.871 (15)	3.873 (11)	3.879 (13)
V(tetracontatetrahedron), Å^3	82.1 (3)	80.0 (4)	79.3 (1)	83.9 (6)
Av lel-lel dist, Å	2.48 (5)	2.54 (24)	2.66 (18)	2.74 (4)
Av ob-ob dist, Å	2.29 (9)	2.47 (13)	2.62 (20)	2.91 (5)

[a] Reference 33. [b] Reference 30. [c] Reference 34. Values in parentheses are the root-mean-square average of the esd for each measurement.

the metal ion to each of the 44 triangular planes. The total volume of the tetracontatetrahedron is obtained from the sum of the volumes of the 44, nonoverlapping trigonal pyramids.[36] The volume of the polyhedron does not represent the true volume of the cation since the protons are taken as points on the surface which neglects the van der Waals contact quasihemisphere of each proton that extends beyond the polyhedron. Nevertheless, an assessment of the relative volumes of the four isomers can be obtained from this procedure.

The volume listed for each isomer in Table VIII shows that there is no significant difference in the cation size for the four isomers. Thus, the *size* of the counterion should have no influence on the isomer found in the solid state for any given system. This is supported experimentally by the recent report of the structure of $[Cr(en)_3][MoO(OH)(CN)_4] \cdot H_2O$[33] which has a large complex anion in the presence of a $\Lambda\delta\delta\delta$ cation.

Previous workers have claimed that the *structure* of the anion can influence the occurrence of a particular isomer because of the differences in the amine proton arrangements in each of the cation configurations. It was suggested[4] that a large amount of hydrogen bonding was not possible in the $\Lambda\delta\delta\delta$ configuration because all three lel protons in this isomer (for example, H1–H3–H11 in Figure 5) are directed toward a common point on the threefold axis. The formation of a hydrogen bond to one of the lel protons would sterically block the other two. In the $\Lambda\lambda\lambda\lambda$ isomer the lel protons point away from the threefold axis in an outward spiral. Thus, all three lel protons are easily capable of interacting with well-separated Lewis base sites. Such an arrangement was found in $[Cr(en)_3][Co(CN)_6] \cdot 6H_2O$[34] where the $\Lambda\lambda\lambda\lambda$ isomer participates in a large number of stabilizing hydrogen bonds.

This hypothesis was revised by Caughlan et al. when they found extensive hydrogen bonding to the $\Lambda\delta\delta\delta$ isomer in the structure of $[Ni(en)_3]SO_4$.[37] In this compound multiple Lewis base sites on the tetrahedral sulfate anions interact simultaneously with the lel protons stabilizing the $\Lambda\delta\delta\delta$ isomer because its lel protons are close together. This revised interpretation was supported by the later structure determinations of $[Co(en)_3]_2(HPO_4)_3 \cdot 9H_2O$[38] and $[Ni(en)_3](H_3C_2O_2)_2 \cdot 2H_2O$,[5] where several Lewis base sites on the anions interact simultaneously with the lel protons of a cation in the $\Lambda\delta\delta\delta$ configuration.

It is interesting to note that in all of these studies the explanations centered exclusively on the dissimilarity of the two orientations of the lel protons and assumed that the changes in the orientations of the ob protons were not as important. Our calculations listed in Table VIII show that as the isomer changes from $\Lambda\delta\delta\delta$ to $\Lambda\lambda\lambda\lambda$ both the average lel–lel (for example, H1–H3 in Figure 5) and the average ob to ob (for example, H2–H5 in Figure 5) proton distances increase. In fact, the increase for the ob protons is more than twice as large. Thus, hydrogen bond acceptor sites which are close together will interact most favorably with both lel and ob protons of the $\Lambda\delta\delta\delta$ isomer. However, if the hydrogen bond acceptor sites are widely separated, then both the lel and ob protons of the isomers with λ rings will interact more strongly.

We have computed the separation distances of Lewis base sites in several anions and these are listed in Table IX. These

Table IX. Separation Distances between Lewis Base Sites in Various Anions, Å

Anion	Distance	Anion	Distance
NO_3^-	2.20	HPO_4^{2-}	2.42
SO_4^{2-}	2.49	$H_3C_2O_2^-$	2.23
$[Ni(CN)_5]^{3-}{}_{sp}$	4.86, 4.20	$[Co(CN)_6]^{3-}$	4.24
$[Ni(CN)_5]^{3-}{}_{tbp}$	4.30, 5.01, 5.12, 5.86	$[Cu_2Cl_8]^{4-}$	3.24, 3.30, 4.38
$[MoO(OH)(CN)_4]^{3-}$	3.83, 4.52	$[Cr(CN)_5NO]^{3-}$	4.65

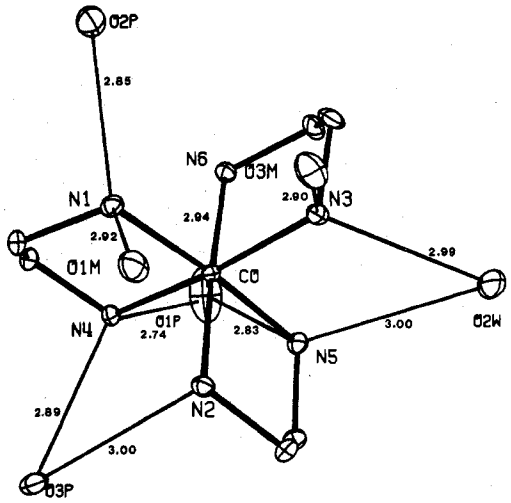

Figure 6. Hydrogen bonding to the $\Lambda\delta\delta\delta$ configuration in $[Co(en)_3]_2(HPO_4)_3 \cdot 9H_2O$.[38] Ellipsoids of 20% probability are used.

anions can be divided into two classes. The oxygen–oxygen distances in small anions like HPO_4^{2-}, SO_4^{2-}, NO_3^-, and $H_3C_2O_2^-$ are never greater than 2.49 Å while the Lewis base site separation distances in larger anions are much longer ranging from 3.24 to 5.86 Å.

The small anions thus have a preference for the $\Lambda\delta\delta\delta$ configuration because maximum hydrogen bonding to all of their available base sites is achieved only when the amine protons are close together and pointed in common directions. In the crystal structure of $[Ni(en)_3](O_2C_2H_3)_2 \cdot 2H_2O$[5] the anion is located along the C_3 axis of the cation and simultaneous hydrogen bonding to the lel protons by several oxygen atoms results. The two hydrates are also positioned to simultaneously hydrogen bond between two ob protons of the cation. This is also true for $[Co(en)_3]_2(HPO_4)_3 \cdot 9H_2O$,[38] for $[Ni(en)_3]SO_4$[37] and its isomorphous analogue $[Cu(en)_3]SO_4$,[39] and for $[Ni(en)_3](NO_3)_2$[32] in which each nitrate is positioned on the threefold axis so that each oxygen is hydrogen bonded to two lel protons. Figure 6 illustrates how this type of hydrogen bonding is achieved in the structure of $[Co(en)_3]_2(HPO_4)_3 \cdot 9H_2O$. The cation–anion arrangement in the cobalt(III) nitrate analogue, (+)-$[Co(en)_3](NO_3)_3$,[40] is not quite as symmetric and the tendency for nitrate to simultaneously form hydrogen bonds between two lel protons is less dominant in this structure. Illustrations depicting the hydrogen bonding environment of the cation in each of these compounds are available.[19]

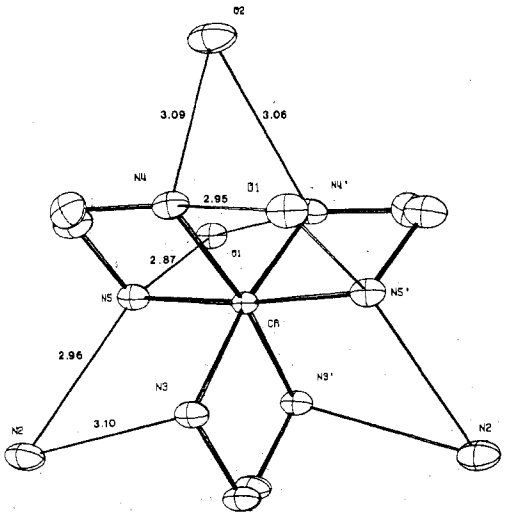

Figure 7. Hydrogen bonding to the $\Lambda\delta\delta\delta$ configuration in $[Cr(en)_3][MoO(OH)(CN)_4]\cdot H_2O$.[33] Ellipsoids of 20% probability are used.

In the $\Lambda\delta\lambda\lambda$ or $\Lambda\lambda\lambda\lambda$ isomers the amine protons are spread farther apart, at distances ranging from 2.42 to 2.91 Å, and they no longer point in a common direction. An anion with large separation distances between Lewis base sites is required to achieve maximum hydrogen bonding to these isomers, since each proton binds to a well-separated hydrogen bond acceptor. For example the cyano group separations on $[Co(CN)_6]^{3-}$ and $[Ni(CN)_5]^{3-}$ can easily span the widest proton–proton separation distance on these cation configurations.

At first glance, compound X in Table VII, $[Cr(en)_3][MoO(OH)(CN)_4]\cdot H_2O$,[33] contradicts the above arguments. This structure exhibits the $\Lambda\delta\delta\delta$ configuration and has several hydrogen bonds to both lel and ob hydrogens. However, the separation distances between Lewis base sites in the Mo(IV) anion are among the largest found in Table IX. The hydrogen bonding network in this structure is presented in Figure 7. Both of the protons within each of the three sets of ob protons are hydrogen bonded to the same acceptor atom, either a cyanide nitrogen or an oxygen. In addition at both the top and the bottom of the cation two lel protons are hydrogen bonded to a single oxygen. It is important to notice that each hydrogen bond acceptor interacts with two protons. This double duty type of bonding draws the amine hydrogens close together and stabilizes the $\Lambda\delta\delta\delta$ configuration.

By contrast we can examine the analogous drawing of the hydrogen bonding in $[Cr(en)_3][Co(CN)_6]\cdot 6H_2O$[34] presented in Figure 8. Here the cation exhibits the $\Lambda\lambda\lambda\lambda$ configuration which has the largest hydrogen–hydrogen separation distances. Several Lewis base sites surround the cation and six of ten of these form only a single hydrogen bond to one of the amine protons. The overall effect is that the hydrogens remain well separated and thus the $\Lambda\lambda\lambda\lambda$ configuration is stabilized in this structure.

The structural details in other compounds involving large anions support these arguments. All of them exhibit the $\Lambda\delta\lambda\lambda$ configuration and none of them have the type of orientation of the Lewis base sites illustrated for $[Cr(en)_3][MoO(OH)(CN)_4]\cdot H_2O$ in Figure 7. For example, the hydrogen bonding environment of the $\Lambda\delta\lambda\lambda$ configuration in the structure of $[Co(en)_3][Cr(CN)_5NO]\cdot 2H_2O$[44] is illustrated in Figure 9. The orientation of the anions in this structure places the Lewis base sites in several different directions around the cation and each of these forms only a single hydrogen bond. Similar illustrations of the other two examples of the $\Lambda\delta\lambda\lambda$ configuration also have been provided.[19] The positions that the large anions in these structures take up are a result of the packing

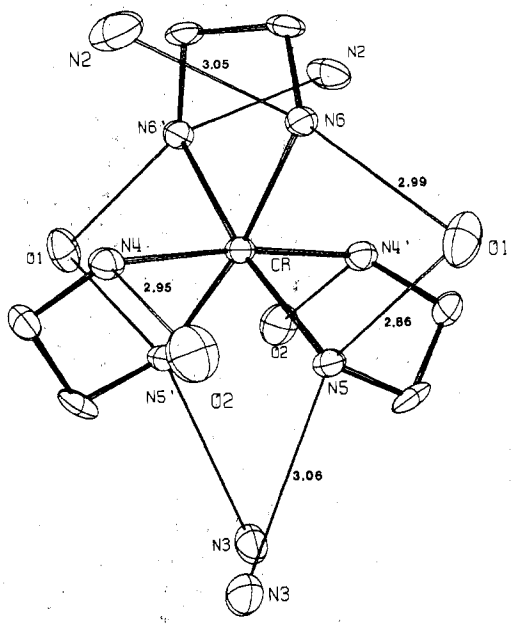

Figure 8. Hydrogen bonding to the $\Lambda\lambda\lambda\lambda$ configuration in $[Cr(en)_3][Co(CN)_6]\cdot 6H_2O$.[34] Ellipsoids of 20% probability are used.

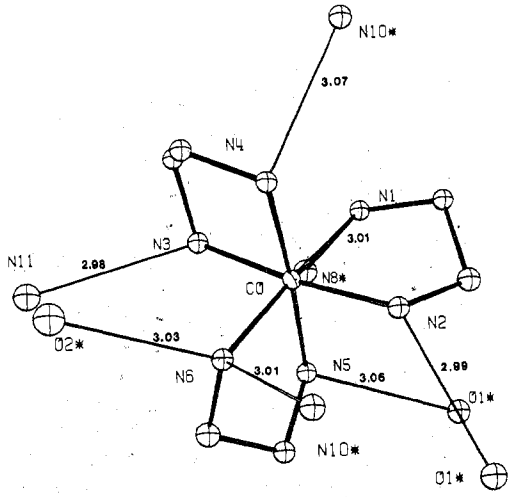

Figure 9. Hydrogen bonding to the $\Lambda\delta\lambda\lambda$ configuration in $[Co(en)_3][Cr(CN)_5NO]\cdot 2H_2O$.[44] Ellipsoids of 20% probability are used.

arrangements in each unit cell and there is no way of predicting the anion–cation orientations of a given compound. It is clear, though, that large anions with widely separated acceptor sites will most usually stabilize either the $\Lambda\delta\lambda\lambda$ or $\Lambda\lambda\lambda\lambda$ configuration.

We have also provided figures which illustrate[19] the hydrogen bonding to the $\Lambda\delta\delta\delta$ cations in $(+)\text{-}[Co(en)_3]Br_3\cdot H_2O$,[41] $(+)\text{-}[Co(en)_3]Cl_3\cdot H_2O$,[42] and $[Co(en)_3]Cl_3\cdot 3H_2O$.[43] Each of the hydrogen bond acceptors in these compounds has only a single atom that can interact with the amine protons. We would expect the protons to be orientated in common directions so that they would all point toward these solitary sources of stabilizing hydrogen bonds. The effect is a preference for the $\Lambda\delta\delta\delta$ configuration which affords the necessary geometry for the amine protons. This is quite obvious in Figure 10 for the bromide compound. Two bromide ions lie very nearly on the C_3 axis above and below the cation thus nearly interacting simultaneously with all six lel protons. Moreover, each pair of ob protons is directly bonded either to a bromide ion or to a hydrate in the same arrangement that we have concluded constrains the protons to lie close together and thus stabilizes the $\Lambda\delta\delta\delta$ isomer.

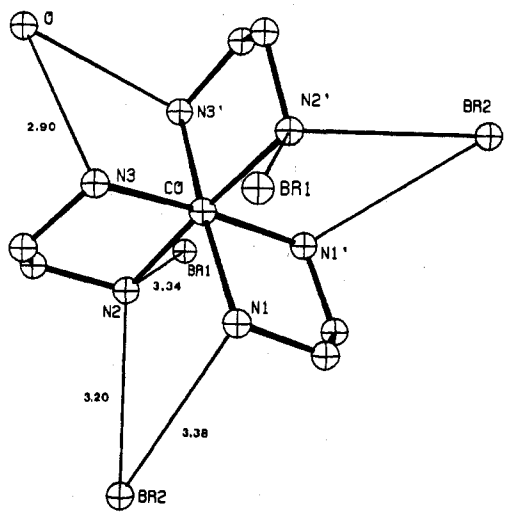

Figure 10. Hydrogen bonding to the $\Lambda\delta\delta\delta$ configuration in (+)-$[Co(en)_3]Br_3 \cdot H_2O$.[41] Ellipsoids of 20% probability are used.

The bromide compound is isostructural with (+)-$[Co(en)_3]Cl_3 \cdot H_2O$[42] and the hydrogen bonding should be identical, but the N1–C12 distance in the chloride analogue at 3.34 Å is slightly longer than the 3.3 Å value normally accepted[31] as the limit for a strong N–Cl hydrogen bond distance. Although this extra long N–Cl distance has been omitted from the survey in Table VII, the (+)-$[Co(en)_3]Cl_3.H_2O$ structure represents another excellent example of the $\Lambda\delta\delta\delta$ isomer stabilized by Lewis base sites positioned between the various sets of amine protons.

The positioning of the chloride ions around the $\Lambda\delta\delta\delta$ isomer in the $[Co(en)_3]Cl_3 \cdot 3H_2O$[43] structure represents a true exception which cannot be explained in view of the observations we have made thus far. Several anions are disturbed in many different directions and the overall appearance would suggest that the $\Lambda\lambda\lambda\lambda$ isomer would be favored in this environment. It is also curious that none of the three hydrate molecules, which we have always found to form good hydrogen bonds in the other $[M(en)_3]^{m+}$ complexes, interacts with the cation in this structure.

Conclusion

Even with this exception we feel we have been able to identify some of the general trends that exist in the hydrogen bonding of $[M(en)_3]^{m+}$ compounds. Our earlier prediction[7] of the mixed ring conformation, $\Lambda\delta\delta\lambda$, in $[Ni(en)_3][B(C_6H_5)_4]_2 \cdot 3(CH_3)_2SO$ has been verified by the x-ray crystallographic data in this work. This should substantiate the use of the previously described spectroscopic technique for the characterization of other $[M(en)_3]^{m+}$ cations of unknown configuration.

The results of this structure indicate that the $\Lambda\delta\delta\lambda$ configuration is the lowest energy isomer. The next higher energy isomer is probably $\Lambda\delta\delta\delta$. It occurs in two-thirds of the reported structures presumably because it is the configuration most easily stabilized by hydrogen bonds. Conversely, the solitary example of the $\Lambda\lambda\lambda\lambda$ configuration indicates that it is the highest energy isomer. Also, the large number of strong hydrogen bonds found with the $\Lambda\lambda\lambda\lambda$ structure support this assignment. The results for $\Lambda\delta\lambda\lambda$ are a bit ambiguous. There are only three known examples of this configuration. This relative rarity warrants placing the $\Lambda\delta\lambda\lambda$ configuration as the second highest energy isomer and in agreement with this the illustration in Figure 9 indicates that rather extensive hydrogen bond stabilization accompanies this example of the $\Lambda\delta\lambda\lambda$ cation in the structure of $[Co(en)_3][Cr(CN)_5NO] \cdot 2H_2O$.[44] However, the $\Lambda\delta\lambda\lambda$ cation of $[Co(en)_3]_2[Cu_2Cl_8]Cl_2 \cdot 2H_2O$[45] is present in a rather weak hydrogen bonding environment only slightly stronger than that found in the two examples of the $\Lambda\delta\delta\lambda$ configuration. The $R(\ln 3)$ entropy advantage of this isomer makes it a probable choice to be at least as stable as the $\Lambda\delta\delta\delta$ configuration. We thus propose the following ordering of the relative free energies of the four unique Λ configuration isomers: $\delta\delta\lambda < \delta\delta\delta \leq \delta\lambda\lambda < \lambda\lambda\lambda$.

Acknowledgment. Computer time on the IBM 370/158 was provided by the University of Hawaii.

Registry No. $[Ni(en)_3][B(C_6H_5)_4]_2 \cdot 3(CH_3)_2SO$, 64872-65-7.

Supplementary Material Available: Table XI, listing the structure factor amplitudes for $[Ni(en)_3][B(C_6H_5)4]_2 \cdot 3(CH_3)_2SO$, and Figures 11 through 19, showing the hydrogen bonding to the cations in $[Ni(en)_3](O_2C_2H_3)_2 \cdot 2H_2O$,[5] $[Ni(en)_3]SO_4$,[37] $[Cu(en)_3]SO_4$,[39] $[Ni(en)_3](NO_3)_2$,[32] (+)-$[Co(en)_3](NO_3)_3$,[40] $[Cr(en)_3][Ni(CN)_5] \cdot 1.5H_2O$,[30] $[Co(en)_3]_2[Cu_2Cl_8]Cl_2 \cdot 2H_2O$,[45] (+)-$[Co(en)_3]Cl_3 \cdot H_2O$,[42] and $[Co(en)_3]Cl_3 \cdot 3H_2O$,[43] respectively (25 pages). Ordering information is given on any current masthead page.

References and Notes

(1) This paper is abstracted from a dissertation submitted to the Graduate Division of the University of Hawaii by J.T.H. in partial fulfillment of the requirements for the Doctor of Philosophy Degree in Chemistry.
(2) *Inorg. Chem.*, **9**, 1 (1970).
(3) E. J. Corey and J. C. Bailar, Jr., *J. Am. Chem. Soc.*, **81**, 2620 (1959).
(4) K. N. Raymond, P. W. R. Corfield, and J. A. Ibers, *Inorg. Chem.*, **7**, 842 (1968).
(5) R. E. Cramer, W. Van Doorne, and J. T. Huneke, *Inorg. Chem.*, **15**, 529 (1976).
(6) J. R. Gollogly, C. J. Hawkins, and J. K. Beattie, *Inorg. Chem.*, **10**, 317 (1971).
(7) R. E. Cramer and J. T. Huneke, *Inorg. Chem.*, **14**, 2565 (1975).
(8) S. F. Pavkovic and D. W. Meek, *Inorg. Chem.*, **4**, 20 (1965).
(9) E. Hilti, ABSCOR Computer program, Chemistry Department, University of Hawaii, 1975; T. Dahl, ABSCO computer program, Chemistry Department, University of Oslo, modified by T. Ottersen, 1973, and E. Hilti, 1975.
(10) R. E. Cramer, W. Van Doorne, and R. Dubois, *Inorg. Chem.*, **14**, 2462 (1975).
(11) "International Tables for X-Ray Crystallography", Vol. III, Kynoch Press, Birmingham, England, 1962, p 201.
(12) R. F. Stewart, E. R. Davidson, and W. T. Simpson, *J. Chem. Phys.*, **42**, 3178 (1965).
(13) Reference 11, p 215.
(14) G. H. Stout and L. H. Jensen, "X-Ray Structure Determination", Macmillan, New York, N.Y., 1968, p 277.
(15) J. T. Huneke, FSHARP Computer Program, Chemistry Department, University of Hawaii, 1975.
(16) K. Seff, HFIND Computer Program, Chemistry Department, University of Hawaii, 1971.
(17) M. R. Churchill, *Inorg. Chem.*, **12**, 1213 (1973).
(18) W. C. Hamilton, "Statistics in Physical Science", Ronald Press, New York, N.Y., 1964, pp 157–162.
(19) See paragraph at end of paper regarding supplementary material.
(20) L. J. Guggenberger and R. A. Jacobson, *Inorg. Chem.*, **7**, 2257 (1968).
(21) R. E. Cramer, *Inorg. Chem.*, **11**, 1019 (1972).
(22) D. M. Duggan and D. N. Hendrickson, *Inorg. Chem.*, **13**, 2056 (1974).
(23) M. Bacci and C. A. Chilardi, *Inorg. Chem.*, **13**, 2398 (1974).
(24) Y. Kojima, M. Matsui, and K. Matsumoto, *Bull. Chem. Soc. Jpn.*, **48**, 2192 (1975).
(25) D. Viterbo, *Acta Crystallogr., Sect. B*, **31**, 2151 (1975).
(26) R. Thomas, C. B. Shoemaker, and K. Eriks, *Acta Crystallogr.*, **21**, 12 (1966).
(27) M. A. Viswamitra and K. K. Kannan, *Nature (London)*, **209**, 1016 (1966).
(28) C. C. Levin, *J. Am. Chem. Soc.*, **97**, 5649 (1975).
(29) L. Pauling, "The Nature of the Chemical Bond", Cornell University Press, Ithaca, N.Y., 1960, p 257.
(30) K. N. Raymond, P. W. R. Corfield, and J. A. Ibers, *Inorg. Chem.*, **7**, 1362 (1968).
(31) W. C. Hamilton and J. A. Ibers, "Hydrogen Bonding in Solids", W. A. Benjamin, New York, N.Y., 1968.
(32) L. N. Swink and M. Atoji, *Acta Crystallogr.*, **13**, 639 (1960).
(33) P. R. Robinson, E. O. Schlemper, and R. K. Murmann, *Inorg. Chem.*, **14**, 2035 (1975).
(34) K. N. Raymond and J. A. Ibers, *Inorg. Chem.*, **7**, 2333 (1968).
(35) T. Ottersen, MOLGE Computer program, Chemistry Department, University of Hawaii, 1973.
(36) L. Lines, "Solid Geometry", Dover Publications, New York, N.Y., 1965, p 75.
(37) M. ul-Haque, C. N. Caughlan, and K. Emerson, *Inorg. Chem.*, **9**, 2421 (1970).
(38) E. N. Duesler and K. N. Raymond, *Inorg. Chem.*, **10**, 1486 (1971).
(39) D. L. Cullen and E. C. Lingafelter, *Inorg. Chem.*, **9**, 1858 (1970).
(40) D. Witiak, J. C. Clardy, and D. S. Martin, Jr., *Acta Crystallogr., Sect. B*, **28**, 2694 (1972).
(41) K. Nakatsu, *Bull. Chem. Soc. Jpn.*, **35**, 832 (1962).

(42) M. Iwata, K. Nakatzu, and Y. Saito, *Acta Crystallogr., Sect. B*, **25**, 2562 (1969).
(43) K. Nakatsu, Y. Saito, and H. Kuroya, *Bull. Chem. Soc. Jpn.*, **29**, 428 (1956).
(44) J. H. Enemark, M. S. Quinby, L. L. Reed, M. J. Steuck, and K. K. Walthers, *Inorg. Chem.*, **9**, 2397 (1970).
(45) D. J. Hodgson, P. K. Hale, and W. E. Hatfield, *Inorg. Chem.*, **10**, 1061 (1971).

Contribution from the Laboratoire de Chimie des Mêtaux de Transition and Laboratoire de Spectrochimie du Solide, Université Pierre et Marie Curie, 75230 Paris Cedex 05, France

Structure and Properties of the Mixed-Valence $[W_4O_8Cl_8(H_2O)_4]^{2-}$ Ion

YVES JEANNIN,*[1] JEAN-PIERRE LAUNAY,[1] JACQUES LIVAGE,[2] and ALEXANDRA NEL[1]

Received May 5, 1977

The crystal structure of the mixed-valence W^V/W^{VI} salt $[HNMe_3]_2[W_4O_8Cl_8(H_2O)_4]\cdot 2H_2O$ has been determined from three-dimensional x-ray data collected by counter techniques with Mo Kα radiation. The structure was refined by full-matrix least-squares methods, using 833 observed independent reflections, to a conventional weighted R factor of 0.034. Crystal data are as follows: orthorhombic, space group *Ccca*, $a = 11.42$ (1) Å, $b = 22.84$ (1) Å, $c = 11.80$ (1) Å, $Z = 4$. The $W_4O_8Cl_8(H_2O)_4^{2-}$ ion is formed by the association of four $WO_3Cl_2(H_2O)$ octahedra sharing corners. The four W atoms form a nearly planar square and are joined through linear oxygen bridges. Each W atom is displaced toward a terminal unshared oxygen atom and is thus found alternately 0.18 Å above or below the molecular plane. Although metal atoms are crystallographically equivalent, the complex must be considered as containing 2 W^V and 2 W^{VI}, as shown by ESCA and especially ESR studies. The latter technique reveals the existence of an intramolecular electronic exchange (hopping) occurring at a rate of ca. 10^8 Hz at −50 °C. The electronic spectrum is also discussed.

Introduction

Mixed-valence compounds contain ions of the same element in different formal oxidation states.[3,4] This yields new properties which may not be the sum of those due to the isolated constituents in their pure oxidation states; in particular, magnetic and optical behavior, as well as electronic conductivity, can be drastically modified.

Robin and Day[3] proposed a classification of these compounds, according to the more or less delocalized character of valence electrons. Class I includes those compounds in which valences are so firmly trapped that no interaction occurs and their properties are just the sum of the properties of their components. On the other hand, class III compounds exhibit a complete delocalization of valence electrons via polycentric molecular orbitals, and no integer oxidation states can be ascribed to the constitutive metal ions. Intermediate cases are referred to as class II, where there is only a slight delocalization in the ground state, and, as a first approximation, different integral oxidation states can be ascribed to the constitutive elements. However, a valence exchange can occur through two mechanisms:[5] (i) by light absorption, generally in the visible part of the spectrum (intervalence transfer absorption) and (ii) by thermal exchange which constitutes an internal homonuclear redox reaction (hopping).

The distinction between class II and III mixed-valence complexes is commonly based upon the existence or nonexistence of distortions of the metal–ligand bonds induced by the change in the oxidation state.[6,7] In class II compounds, these distortions are present; for instance, metal–ligand distances are longer for the lower oxidation state, and the valence electrons are thus self-trapped since metallic sites are no longer equivalent. On the contrary, for class III compounds, all sites are strictly equivalent giving rise to a full delocalization of the valence electrons.

A number of mixed-valence compounds can be obtained from molybdenum or tungsten, especially between oxidation state V and oxidation state VI. A mixed anion, formulated as $W_4O_8Cl_8^{2-}$ with formally 2 W^V and 2 W^{VI}, has been prepared by one of us.[8] It can be obtained upon addition of sodium tungstate to a concentrated solution of W^V in 8–12 M HCl. Reaction 1 occurs, the equilibrium being displaced

$$2WO_2Cl_4^{2-} + 2WOCl_5^{2-} + 2H_2O \leftrightarrows W_4O_8Cl_8^{2-} + 4H^+ + 10Cl^- \quad (1)$$

toward the left. However, by means of selective precipitation, the mixed-valence compound can be obtained free from its constituents.

This paper deals with structural and spectroscopic studies of the trimethylammonium salt $[W_4O_8Cl_8(H_2O)_4]\cdot(HNMe_3)_2\cdot 2H_2O$. The pyridinium salt, which was isolated and crystallized first, appeared to be unsuitable for an x-ray structural determination, presumably as a result of crystallographic disorder.

Experimental Section

Preparation of Crystals. A ca. 0.15 M W^V solution in 12 M HCl was prepared according to a method already described.[8] W^{VI} was then added as powdered $Na_2WO_4\cdot 2H_2O$ in stoichiometric amount, with vigorous stirring. The reaction mixture was kept at 0 °C for 2–3 days, in order to shift the equilibrium toward the right.[8] A mixture of blue oxides and sodium chloride precipitated and was filtered off. The addition of trimethylammonium chloride at ca. 0.02 M concentration to the dark blue solution gave rise to a slow (1 day) crystallization.

As an alternative procedure, trimethylammonium chloride was added at a 0.04 M final concentration to the W^V solution. The mixture was slowly oxidized by atmospheric oxygen, for instance, by keeping it in a loosely stoppered flask. The W^V–W^{VI} complex slowly appeared as crystals after a few days. Anal. Calcd for $[W_4O_8Cl_8(H_2O)_4]\cdot[HN(CH_3)_3]_2\cdot 2H_2O$: W, 53.48; Cl, 20.62; C, 5.23; N, 2.03. Found: W, 52.59; Cl, 20.67; C, 5.14; N, 2.02.

X-Ray Studies. The crystals were in the form of tangled tablets but monocrystalline samples could be obtained by cleavage. A trapezoidal-based prism was set in a Pyrex tube with its 101 axis along the rotation axis and sealed under argon, the x-ray path length ranging from 0.25 to 0.1 mm.

The unit cell was found orthorhombic by the precession method using Mo Kα radiation (0.71069 Å). Lattice constants were measured on films, using a binocular with micrometric film translations. Cell parameters obtained were $a = 11.42$ (1) Å, $b = 22.84$ (1) Å, and $c = 11.80$ (1) Å.

Systematic extinctions, $h + k = 2n$ for all reflections, $l = 2n$ for $0kl$ and $h0l$, and $h = 2n$ for $hk0$, unambiguously designated the space

0020-1669/78/1317-0374$01.00/0 © 1978 American Chemical Society